Magnetospheric Plasma Modeling (0-100 keV)

Henry Berry Garrett and Guy C. Spitale
Jet Propulsion Laboratory, California Institute of Technology, Pasadena, California

Introduction

BECAUSE spacecraft surface charging is primarily a current balance phenomenon, it in general a function of the dominant currents to and from the vehicle's surface. Within the near-Earth magnetosphere the dominant currents to the surface are the ambient space plasma fluxes between approximately 0 and 100 keV. Considering the relative accessibility and the scientific interest in this plasma population, one would expect that much would be known about this important source of spacecraft charging. However, it is only in the last decade that a clear picture of this environment has emerged. This is the result of a variety of both physical and theoretical difficulties. Physically, accurate low-energy particle detectors have been developed and flown to any great extent in the near-Earth environment[1] only within the last decade. The development of low-energy particle models has had to await the advance of accurate electric field models. Unlike the high-energy radiation environment, where engineering interest in radiation damage provided a strong impetus, until recently, there was little practical reason to study the low-energy plasma. In fact, a major effort to understand this environment was initiated only when spacecraft charging became a major issue and it was realized that this environment could have a significant effect on spacecraft systems. Coupled with the recent growth in observations and the improvements in electric and magnetic field models, this has generated a burst of interest and quantitative improvement in the modeling of the near-Earth, low-energy plasma population. Therefore, the intent of this paper is to summarize the basic features of the models that have resulted from that burst of activity.

In the next section, four categories of models, based primarily on the degree of empirical and theoretical input and in part of the potential users, will be delineated. Different levels of modeling and potential problem areas will be covered systematically with the intent of providing both a review of current activities and a practical user's guide of such models. The general division of the magnetospheric population into four domains (Fig. 1), as suggested by Vasyliunas,[3] will be adopted throughout this paper, providing a means of dividing the magnetosphere into regions based on dominant physical characteristics and hence a means of selecting a model relevant to the user's needs. In terms of this division, there is first the plasmasphere, considered an extension of the ionosphere, termed the ionospheric domain. Beyond it lies the region populated by fluxes of kiloelectron volt particles associated with the plasma sheet and closely coupled with geomagnetic substorms called the auroral domain. This is the region of greatest concern for spacecraft charging. At higher latitudes lies the third region, marked by very low particle densities, termed the polar cap domain. The stably trapped energetic particles populating the radiation belts, which overlay the other regions, make up the fourth and final domain, the Van Allen domain. Although these radiation particles (energies in excess of 100 keV), through the process of charge deposition, are a principal source of spacecraft charging, they are not thought to contribute significantly to surface charging and will not be discussed further. The paper will concentrate rather on the ionospheric and auroral domains, that is, roughly, the particle population below 100 keV and between an altitude of 200 km and 10 Earth radii (R_E). The polar cap domain will be

---

Henry Berry Garrett was born in San Francisco in 1948. He received his undergraduate degree in physics and Ph.D. in space physics and astronomy from Rice University in 1970 and 1973, respectively. Commissioned in the U.S. Air Force, Capt. Garrett spent six years at the Air Force Geophysics Laboratory. He published more than 50 scientific papers and was awarded the Air Force's Harold Brown Award for outstanding scientific achievement. Since 1980 Dr. Garrett has been the lead technologist in spacecraft interactions at the Jet Propulsion Laboratory, serving as research scientist in the Reliability Engineering Section. An internationally recognized authority on spacecraft environments and interactions, he is a member of the AIAA, the American Geophysical Union, the Astronomical Society of America, the American Institute of Physics, and the International Association of Geomagnetism and Aeronomy, of which he is an officer.

Guy C. Spitale was born in Chicago in 1941. He received his B.S. in physics from Louisiana State University in 1963, M.S. in engineering space physics from the Air Force Institute of Technology in 1965, and Ph.D. in engineering applied sciences (nuclear) from the University of California at Davis in 1974. Commissioned in the U.S. Air Force in 1963, he served from 1969 to 1972 as Military Research Associate at Lawrence Livermore Laboratories; from 1972 to 1976 on the physics department faculty at the Air Force Institute of Technology; and from 1976 to 1979 as Chief of the Research Branch, Advanced Technology Division, at the Air Force Technical Applications Center. In 1979 he assumed leadership of the Air Force Armament Laboratory Hydrocode Team. Dr. Spitale is currently Technical Group Supervisor for the Natural Radiation Survivability/Vulnerability Group at the Jet Propulsion Laboratory.

Received Oct. 19, 1984; revision received Jan. 31, 1985.

discussed only briefly, since much of the relevant data, particularly from the Dynamics Explorer (DE) satellite, are still being analyzed.

Types of Quantitative Models

Definitions

Although classification schemes are always imperfect, a meaningful classification of quantitative models can be devised on the basis of the ratio of theoretical to empirical input to the model. By way of illustration, the simplest model conceptually is a statistical compendium or histogram of various parameters as a function of space and time. Such a model has little theoretical input, being based on actual measurements. Consideration of physical principles makes possible the derivation of analytic expressions capable of simulating variations in the environment, the second type of model. The third type of model to be considered is termed a static field model since it employs theory to predict the trajectories or diffusion of particles in static electric and magnetic fields. Finally, the most complete model from a theoretical standpoint is a full, three-dimensional, time-dependent model capable of taking into account particle injection events. Each of these model types will be discussed subsequently.

Statistical Models

Simply stated, statistical models are compendia or histograms of actual data organized in terms of various plasma parameters. The principle difficulty for this class of models is in deciding what plasma parameters are critical for describing the environment. The central concept in such a description of the plasma is the distribution function (a distribution function gives the particle density within a given velocity or, alternatively, momentum increment and spatial volume). Examples are those of Chan et al.,[4] who have generated "average" spectra in terms of energy and differential number flux for several magnetospheric and solar wind regions. The electron and ion distributions for the inner magnetosphere and plasma sheet from Ref. 4 are shown in Fig. 2. Such a simple description is of great value in many applications (e.g., dosage calculations); however, modeling the magnetosphere adequately would require a prohibitive number of spectra as functions of both time and spatial coordinates (see, for example, the geosynchronous models of Su and Konradi[5]). Moreover, the distribution function itself requires a detailed description in terms of energy, composition, and particle pitch angle. The goal of plasma models, therefore, is to provide as much information about the distribution function as concisely as possible. Several such attempts will be covered below.

DeForest and McIlwain[6] simplified the problem for the geosynchronous orbit, making the representation of the plasma distribution function more concise and capable of statistical study, by developing a description of the plasma in terms of the first four moments of the distribution function:

$$\langle \mathrm{ND}_i \rangle = 4\pi \int_0^\infty (v^0) F_i v^2 \, dv = n_i \tag{1}$$

$$\langle \mathrm{NF}_i \rangle = \int_0^\infty (v^1) F_i v^2 \, dv = \left(\frac{n_i}{2\pi}\right)\left(\frac{2kT_i}{\pi m_i}\right)^{1/2} \tag{2}$$

$$\langle \mathrm{ED}_i \rangle = \frac{4\pi m_i}{2} \int_0^\infty (v^2) F_i v^2 \, dv = \frac{3}{2} n_i k T_i \tag{3}$$

$$\langle \mathrm{EF}_i \rangle = \frac{m_i}{2} \int_0^\infty (v^3) F_i v^2 \, dv = \left(\frac{m_i n_i}{2}\right)\left(\frac{2kT_i}{\pi m_i}\right)^{3/2} \tag{4}$$

where $\langle \mathrm{ND}_i \rangle$ is the number density of species i(cm^{-3}); $\langle \mathrm{NF}_i \rangle$ is the number flux for species i ($\mathrm{cm}^{-2}\ \mathrm{s}^{-1}\mathrm{sr}^{-1}$); $\langle \mathrm{ED}_i \rangle$ is the energy density for species i (erg cm^{-3}); and $\langle \mathrm{EF}_i \rangle$ is the energy flux for species i (erg $\mathrm{cm}^{-2}\ \mathrm{s}^{-1}\ \mathrm{sr}^{-1}$). (The plasma pressure $\langle P_i \rangle$ can be derived by multiplying $\langle \mathrm{NF}_i \rangle$ by πq for an omnidirectional flux; q is the charge.)

On the right-hand sides of Eqs. (1 – 4), for the purpose of illustration, the integral results are given assuming the Maxwell-Boltzmann distribution function:

$$F_i(v) = n_i \left(\frac{m_i}{2\pi k T_i}\right)^{3/2} \exp\left(\frac{-m_i v^2}{2kT_i}\right) \tag{5}$$

where n_i is the number density of species i; m_i the mass of species i; T_i the temperature of species i; v the velocity of species i; k the Boltzmann constant; and F_i the distribution function for species i.

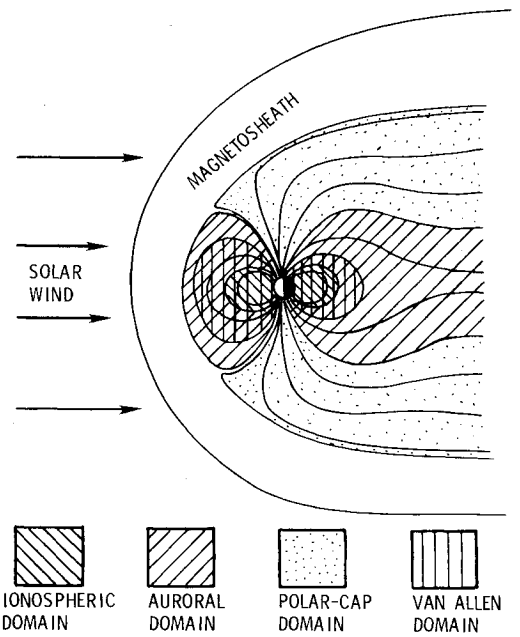

Fig. 1 Noon-midnight meridional cross section of the magnetosphere.[2]

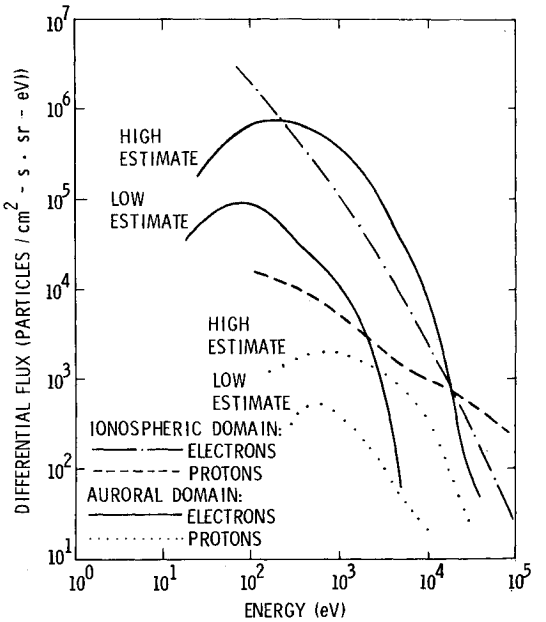

Fig. 2 Plot of the composite electron and proton spectra in the ionospheric and auroral domains.[4]

The description of the plasma in terms of the four moments is particularly appealing from an engineering standpoint because they all have readily comprehensible physical meanings. However, the real value of the technique lies in the fact that they can also be easily used to derive a Maxwell-Boltzmann distribution function approximation to the actual distribution function. In particular, the moments can be used to define a plasma "temperature":

$$T_{av} = \frac{2\langle ED\rangle}{3\langle ND\rangle} \tag{6}$$

$$T_{rms} = \frac{\langle EF\rangle}{\langle NF\rangle} \tag{7}$$

For reference, T_{av} is equal to two-thirds of the mean particle energy. T_{rms}, although often used in the literature, has no real physical meaning unless the state of the plasma can be represented by a single Maxwellian distribution, in which case $T_{av} = T_{rms}$. Typically for the magnetosphere $T_{rms} > T_{av}$. Even so, given one of these temperatures and the number density, one can usually define an appropriate Maxwell-Boltzmann distribution for studying spacecraft charging effects.

The use of the four moments allows the calculation of a variety of other parameters including the determination of the more accurate "two-Maxwellian" (the term "bi-Maxwellian" refers specifically to a plasma with a different plasma temperature along the local magnetic field direction than perpendicular to it—in contrast to the "two-Maxwellian" distribution which has two different temperatures along one direction) distribution function (see Ref. 7 or 8 for derivations of the two-Maxwellian components from the four moments):

$$F_2(v) = \left(\frac{m}{2\pi k}\right)^{3/2}\left[\left(\frac{N_1}{T_1^{3/2}}\right)\exp\left(\frac{-mv^2}{2kT_1}\right) + \left(\frac{N_2}{T_2^{3/2}}\right)\exp\left(\frac{-mv^2}{2kT_2}\right)\right] \tag{8}$$

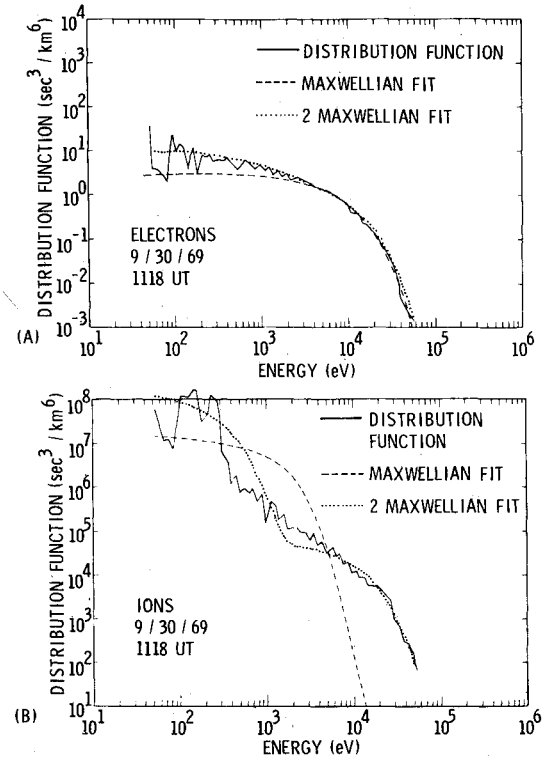

Fig. 3 Electron and ion distribution functions and corresponding Maxwellian and two-Maxwellian fits based on the four moments of the distribution function for actual ATS-5 data.[7]

where N_1 are N_2 are the two population densities (cm^{-3}) and T_1 and T_2 the two population temperatures (eV). Figure 3 demonstrates a two-Maxwellian fit to actual data (the data were selected at random and are not intended to represent typical conditions). As Fig. 3 shows, the two-Maxwellian representation, having four rather than two variables, is a more accurate fit to the actual distribution function than the single Maxwellian representation.

Exhaustive testing of the two-Maxwellian technique[9-11] has revealed that although the majority of plasma spectra may be well fit by the two-Maxwellian function over the 1-100 keV energy range, exceptions are observed because the function can underestimate the flux seriously at energies above a few tens of kiloelectron volts. Such fitting procedures, in lieu of the detailed spectra, must be used with caution. Even so, the great simplicity of the Maxwellian and two-Maxwellian fits and their ready integrability has made them the preferred form of representation of the near-Earth plasma environment for practical spacecraft charging applications. Herein, most of the statistical results will be presented in terms of these moments (and current density) or the Maxwellian fits derived from them. As examples of this procedure, Fig. 4 presents statistical distributions for the current density and temperature for electrons and ions at geosynchronous orbit for several satellites. Table 1 presents related data on the average ion composition for the same region. The most extensive compilation of such parameters can be found in Ref. 14 for the P78-2 spacecraft data set.

Although the plasmasphere, plasma sheet, magnetopause, and solar wind all have been observed to penetrate to geosynchronous orbit at times, one does not obtain a true picture of the near-Earth magnetosphere solely from geosynchronous observerations or a discussion limited to the statistical techniques and results developed for the geosynchronous orbit. In particular, the models discussed previously have not been three dimensional. A somewhat subjective, but useful, three-dimensional model can be constructed by extrapolating the observations of a satellite in an eccentric, moderately inclined orbit in the form of meridional intensity plots of high-energy particles. A particularly good example is the meridian plot[15] in

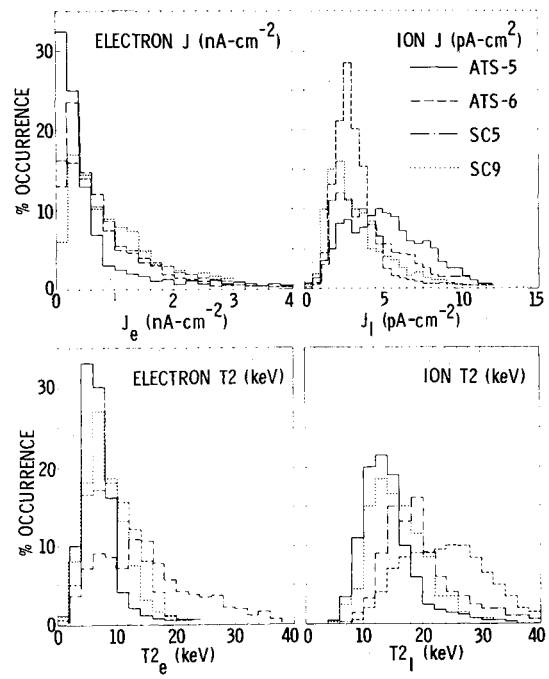

Fig. 4 Comparisons of the statistical occurrence frequencies of the electron and ion current flux (J) and two-Maxwellian temperature (T2) for the ATS-5 and -6 spacecraft and the P78-2 instruments SC5 and SC9.[9]

Fig. 5 in generalized $R-\lambda_m$ coordinates for ions in the 200 eV-50 keV range (see Ref. 16 for an explanation of geophysical coordinate systems). Plots for the other plane (i.e., plots of the moments as functions of local time and radial position in the equatorial plane) have been made from the SCATHA data between 5 and $8R_E$.[14]

As early as 1966, Carpenter,[17] using ground-based ionospheric whistler studies, delineated the approximate shape and density of the plasmaspheric electron population (Figs. 1 and 6). These results demonstrated that the low-energy, near-Earth plasmasphere's characteristics are linked closely to the Earth's ionosphere.[18-21] Although observations of the asymmetry between the positions of the noon and midnight plasmapauses[22] and the deviation of the plasma trough (or region of plasma depletion) at midlatitudes from the equatorial plasmapause[23] cast doubt on the simple statistical representation given by Figs. 1 and 6, the model is quite adequate for describing the average structure of the ionospheric domain for the purposes of spacecraft charging studies.

At low altitudes (< 1000 km) the plasmasphere merges with the ionosphere. As shown in Figs. 7-11, the vertical structure of the plasma becomes quite complex, being divided into many different levels based on where the various inflections in density occur (i.e., the D, E, and F layers). Crude, statistically averaged profiles as shown in these figures[24] are the most frequently used inputs for modeling this region. As will be seen in the next section, however, more sophisticated models are now available that provide considerably more information on this complex structure.

Analytic Models

The major difficulty with statistical models is their inability to simulate the effects of complex time variations while maintaining the proper relationships between all of the parameters necessary to describe the plasma. For the geosynchronous orbit, DeForest and Wilson[25] have tackled this problem by interpolating actual data provided on computer tapes from ATS-5 for representative intervals of geomagnetic activity. This method, although it is precise and explicitly includes time variations, lacks compactness and does not directly provide many of the plasma parameters (such as number density or number flux) often needed for spacecraft charging applications. As a solution to this problem of tradeoffs between accuracy and massive databases, analytic equations capable of modeling specific parameter variations have been developed.

As a first example, Mauk and McIlwain[26] developed an analytic expression for the evening-midnight injection boundary Lb (in units of R_E), the boundary along which "hot" plasma appears at and near geosynchronous orbit at the beginning of a substorm. In terms of local time (LT) and the geomagnetic index K_p the model predicts:

$$Lb = (122 - 10\,K_p)/\mathrm{LT} - 7.3) \tag{9}$$

(Since high surface potentials are often observed when a satellite crosses this boundary, it is of particular importance to the spacecraft charging modeler.) This formula is derived from ATS-5 data and is based in part on a formula for the plasmapause position Lpp (in R_E) in the midnight-dawn sector from Ref. 19 (see also Refs. 27-30):

$$Lpp = 5.7 - 0.47\,K_p \tag{10}$$

(as K_p is taken to be the maximum value in the preceding 12 h in the Carpenter-Park formula and the instantaneous value in

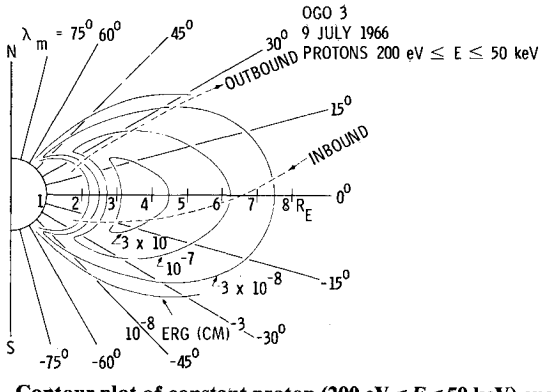

Fig. 5 Contour plot of constant proton (200 eV ≤ E ≤ 50 keV) energy densities in the R-λ_m coordinate system on July 9, 1966.[15]

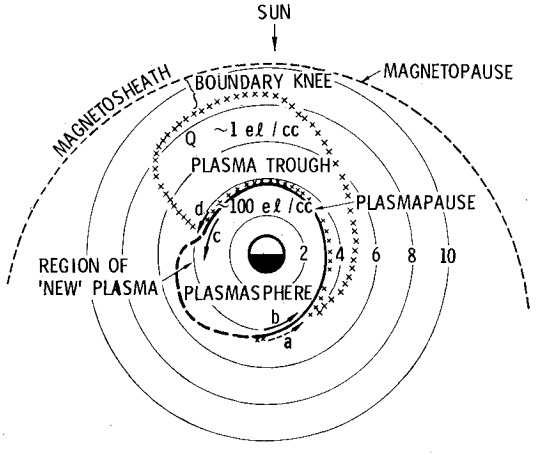

Fig. 6 Equatorial cross section of the magnetosphere illustrating the approximate locations of the plasmasphere and plasma trough in local time and Earth radii.[17]

Table 1 Average ion composition between approximately $L = 6.9$ and 8.2 and in the energy per charge range 1-16 keV/e. The data are based on six 2-h periods[12,13]

	Average ion composition							
	Number density, 10^{-2} cm^{-3}				Average total energy, keV			
	H^+	He^{++}	He^+	O^+	H^+	He^{++}	He^+	O^+
				Storm dayside				
Average	57	1.1	0.8	15	6.0	11.8	5.1	4.7
Range	20 – 120	0.2 – 3.6	0.4 – 1.2	2.1 – 30	5.0 – 8.5	10.2 – 18.8	3.9 – 7.3	4.1 – 6.1
				Storm nightside				
Average	59	1.0	0.7	11	6.2	14.5	4.2	4.3
Range	25 – 135	0.6 – 1.5	0.3 – 1.8	3 – 22	3.6 – 9.6	10.2 – 20.2	2.8 – 5.0	3.9 – 4.9
				Magnetic quiet				
Average	15	0.1	0.4	0.9	6.8	13.9	5.8	5.1
Range	8.2 – 25	0.02 – 0.2	0.2 – 0.6	0.1 – 1.6	5.4 – 8.6	9.0 – 19.6	3.8 – 8.6	3.8 – 7.2

the Mauk-McIlwain formula, these equations should be treated as rough approximations). As will be shown later, these equations are not only important for predicting when a vehicle is likely to pass into a potentially high charging environment or into the plasmasphere but may also be used as the basis for much more sophisticated models of the magnetosphere.

Several simple analytic expressions for describing geosynchronous plasma distribution functions have also been developed. Su and Konradi,[5] for example, elected to fit yearly averages of the distribution function derived from ATS-5 data with a power law in energy as a function of local time and geomagnetic activity. A more compact representation is provided by Garrett and DeForest[8] who fit the first four moments of the plasma distribution function for 10 selected days of ATS-5 data with an equation linear in the geomagnetic index A_p and varying diurnally and semidiurnally in local time:

$$M_i(A_p, \mathrm{LT}) = (a_0 + a_1 A_p)\ \{b_0 + b_1 \cos[(2\pi/24)\ (\mathrm{LT} + t_1)]$$
$$+ b_2 \cos[(4\pi/24)\ (\mathrm{LT} + t_2)]\} \qquad (11)$$

where M_i is the moment i, A_p the daily average of a_p, and a_0, a_1, b_0, b_1, b_2, t_1, and t_2 fitted parameters.[8] The days were selected so that a wide range of geomagnetic activity was included and a plasma injection was initiated when the ATS-5 satellite was near local midnight.

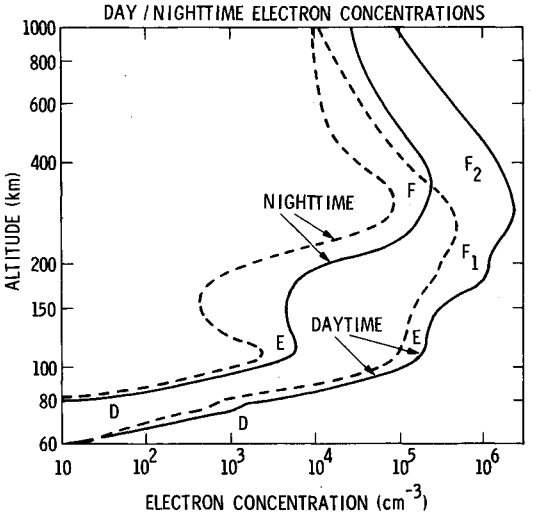

Fig. 7 Typical midlatitude daytime and nighttime electron profiles for sunspot maximum (—) and minimum (– – –).[24]

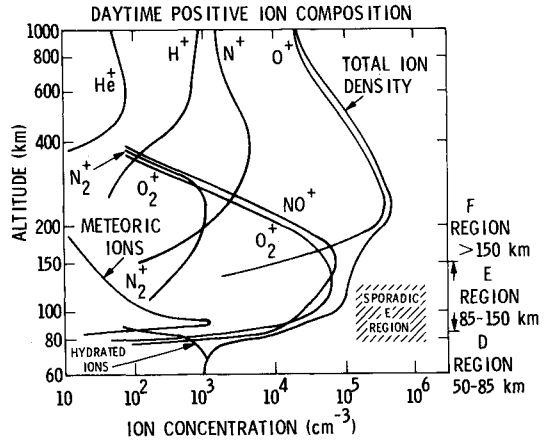

Fig. 8 Typical ion profiles of the midday, midlatitude ionosphere at sunspot minimum.[24]

As discussed previously, given estimates of the four moments, one can readily estimate the plasma temperature, current density, and a single- or two-Maxwellian distribution. Figure 11 compares the variations predicted by this simple analytic formulation for J and T_2 with the actual statistical variations observed. The good agreement lends credibility to this type of representation. At the highest levels of geomagnetic activity, however, the model is biased toward the particular active day studied. Even so, the simulation allows predictions of the geosynchronous parameters and has indeed been used successfully to predict real-time spacecraft charging variations as a function of ground-based geomagnetic activity (as yet it has not been extended to the ion composition data although this could be readily accomplished).

Even though the type of model represented by Eq. (11) and Fig. 12 predicts average levels and local time variations adequately, it fails to model the rapid (i.e., one-half hour) variations associated with geomagnetic storms. This is only partially due to the shortcomings of the modeling process itself. The principal deficiency is, rather, the current inability to measure geomagnetic activity at the ground adequately (K_p, for example, is a 3-h average whereas order of magnitude variations in the plasma can take place in minutes!). For modeling purposes, this inadequacy can be offset partially by averaging the time variations for a number of geomagnetic substorms or injection events at one local time.[10,11] The average variations predicted are useful for spacecraft charge modeling of the electron current and temperature variations following an injection event in the midnight quadrant (see Fig. 13).

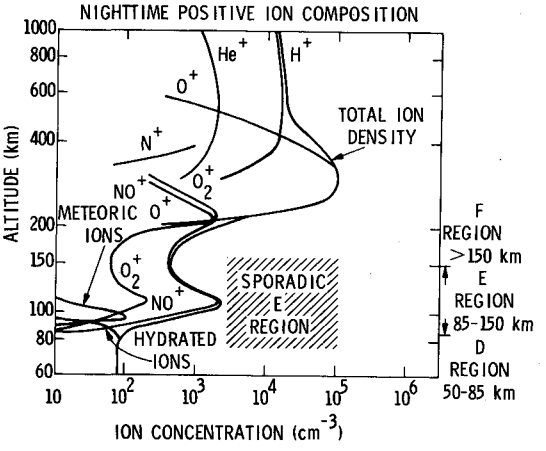

Fig. 9 Typical ion profiles of the nighttime, midlatitude ionosphere at sunspot minimum.[24]

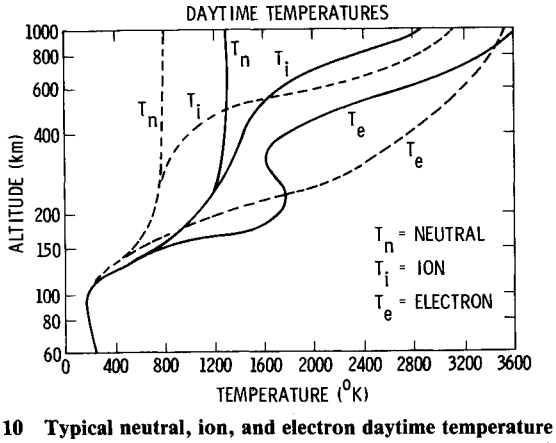

Fig. 10 Typical neutral, ion, and electron daytime temperature profiles at equinox for a midlatitude ionosphere at sunspot maximum (—) and minimum (– – –).[24]

Analytic models of the regimes other than geosynchronous have been developed as well. Good examples of these for the low-altitude ionospheric and polar cap regimes are the phenomenological models of ionospheric electron density developed by Ching and Chiu[31] and Chiu.[32] These models are much more complex but structurally resemble the simple geosynchronous model of Eq. (11). Briefly, Chiu and Ching have used ground measurements of the local time variations in the critical radio frequencies of the ionospheric E, Fl, and F2 regions to estimate the time and spatial variations of total electron density around the world (the critical radio frequency of an ionospheric region or layer, which is easily measured from the ground, is the frequency at which the wave changes from being reflected to transmitted; this frequency is directly proportional to the square root of the electron density at that point). They fit these variations with functions of the independent variables altitude, day of the year (for seasonal effects), geographic and geomagnetic latitude, geomagnetic longitude, geomagnetic dip angle, local time, and sunspot number (for solar cycle effects). Altitude variations are derived, once the maximum density of each region is known, by assuming a Chapman profile for each of the three layers and summing the three densities. Although biased for the particular ionospheric observatories chosen, the model is quite adequate for predicting the average total charge content between 100 and 600+ km (Fig. 14). Magnetic storm effects and other short-term variations are explicitly excluded from the models.

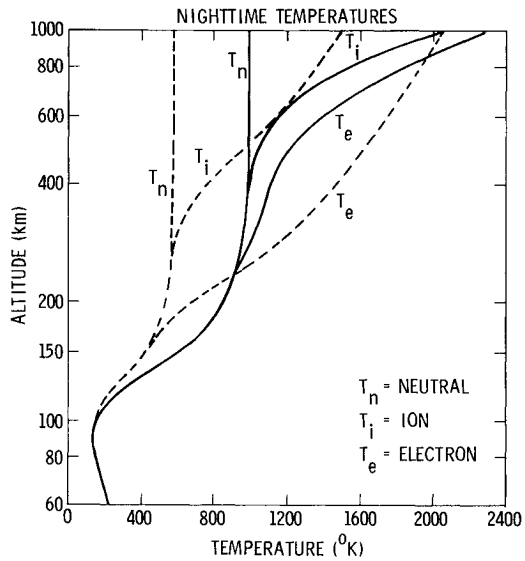

Fig. 11 Neutral, ion, and electron nighttime temperature profiles at equinox for a midlatitude ionosphere at sunspot maximum (—) and minimum (– – –).[24]

The principal analytic ionospheric model available for this lower ionospheric domain is the international reference ionosphere[33] or IRI model. Although of limited accuracy above 200 km, this is the most readily available computer model that gives both electron and ion composition and temperature as a function of longitude, latitude, altitude, sunspot number (R), and time. In this model the bottomside ionosphere is defined in terms of five height regimes, the lowermost of which is subdivided into two regions. In each of these regions the density profiles are fitted to differing analytical representations. These representations vary depending on such factors as whether an F1 layer is present, the existence or nonexistence of the E-region valley, etc.

Figures 15 and 16 show several examples of the output of the IRI model. Figure 15 presents the electron number density and temperature at an altitude of 400 km and sunspot number $R = 100$ in December. The figure shows the electron temperature increasing by a factor of more than 2 in going from the equator to the pole. This is in marked contrast to the behavior of the neutral atmosphere, whose temperature varies by less than 50% for the same conditions. The peaks in neutral and electron densities are both shifted by about 2 h from local noon in response to the Earth's rotation on its axis.

Figure 16, which displays corresponding values for oxygen ion concentration, shows that at 400 km the ionosphere is

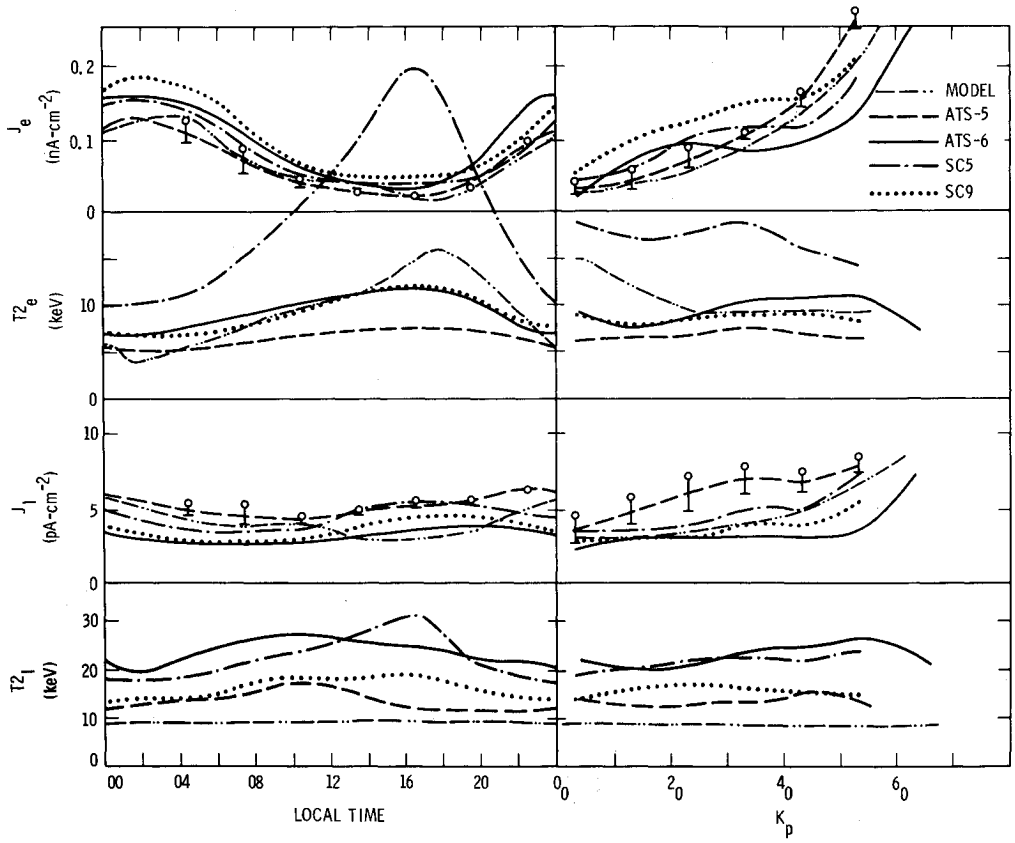

Fig. 12 Average variations in the electron and ion current flux (J) and two-Maxwellian temperature (T2) as functions of local time and geomagnetic index K_p.

dominated by oxygen ions (45% near local midnight and below 30° latitude to 97% over the pole). This is primarily due to the corresponding high level of neutral oxygen. The model assumes that the temperature is the same for all ion species. Unfortunately, although the ion temperature can never exceed the electron temperature for physical reasons, the IRI model occasionally predicts ion temperatures far in excess of the electron temperature. This reflects the fact that the model is based on a limited set of data, particularly for $R < 100$, and needs improvement. The IRI model also has a number of other major defects which include difficulties involved in interfacing the representations of the profiles in adjacent regions and the fact that the auroral enhancement effects are not included in the model. In specific cases the model has been found to give incorrect results due to programming defects. Despite its shortcomings, however, the IRI model still provides the most successful representation of the ionosphere to date and extensive work is being done to improve its database and methods of analytical representation.[34]

The most dramatic changes in the Earth's environment at Shuttle altitudes (~200 km) are brought about by geomagnetic substorms. These changes are reflected in visible auroral displays and intense particle and field variations in the auroral region at Shuttle altitudes. A simple analytical auroral flux model, based on preliminary data provided by the Air Force Geophysics Laboratory (AFGL)[35] and Natonal Oceanic and Atmospheric Administration (NOAA),[36] is presented here to illustrate these effects. The electron number flux and energy flux data were crudely approximated by a simple analytic function in geomagnetic local time and latitude and the geomagnetic K_p index.

The crude model approximated from the AFGL/NOAA flux data was used to estimate the auroral/polar cap electron temperature and number densities. These results are shown in Fig. 17 for the northern winter hemisphere and a K_p of 6_0. They imply that there is a peak in the density of the auroral electron flux of about 1000 cm^{-3} in the noon sector while the auroral electron temperature is 1 keV in the post-midnight sector. Although the validity of this crude result will need to be compared with the actual data when they become available, the range of values should be indicative of the characteristics of the average auroral fluxes at least. Comparisons with other data sources bear this out.

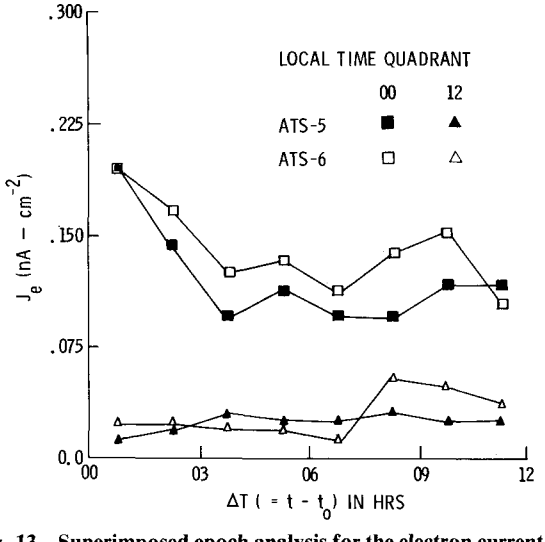

Fig. 13 Superimposed epoch analysis for the electron current flux (J) as a function of time following a substorm injection event.[10]

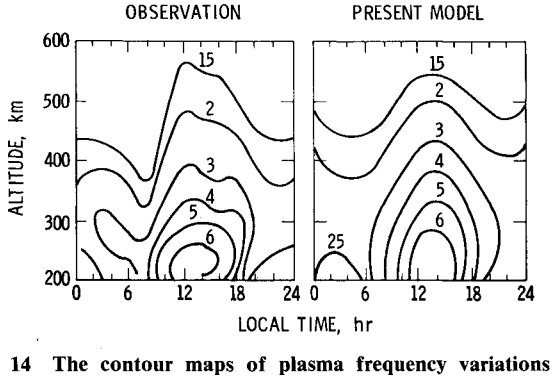

Fig. 14 The contour maps of plasma frequency variations with altitude and local time for November 1964 at Millstone Hill are shown for actual observations and the Ching/Chiu ionosphere model.[31]

Static Models

In general, statistical models and simulations are limited to the regions where extensive observations are available. This means that, whereas the geosynchronous and low-altitude/low-latitude regions (where most scientific satellites

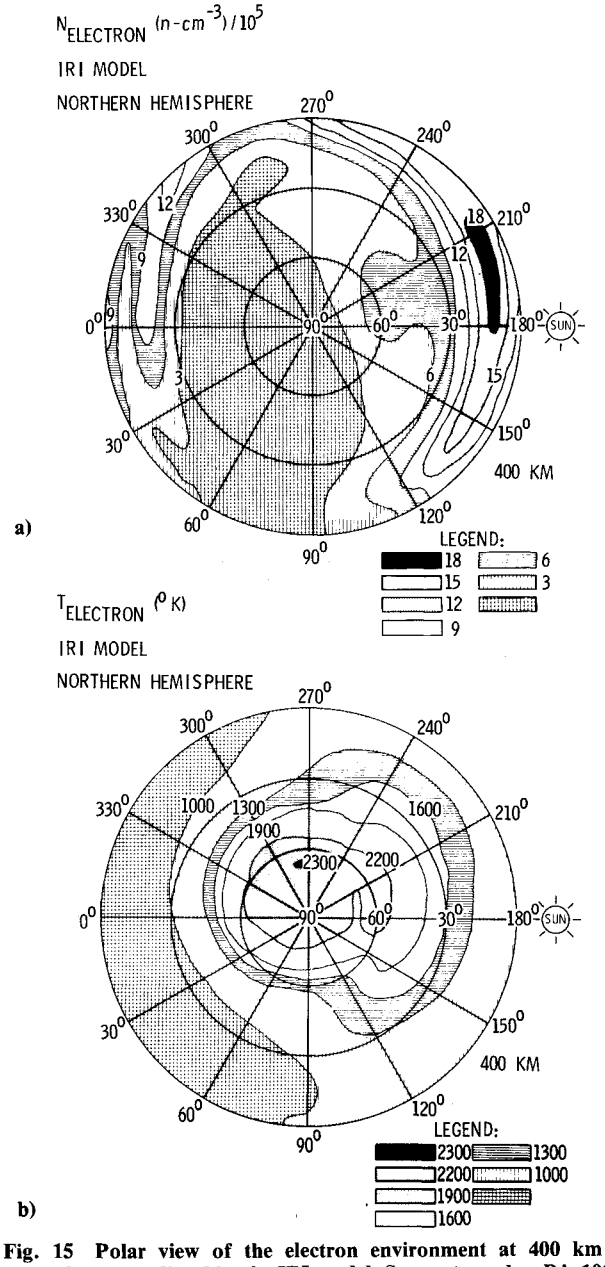

Fig. 15 Polar view of the electron environment at 400 km for December as predicted by the IRI model. Sunspot number R is 100. a) Electron density; b) Electron temperature.

have flown) are adequately described by such techniques, the polar cap, auroral zones, and altitudes between 1000 km and geosynchronous are not. It is possible, however, to extend geosynchronous and low-altitude observations to other latitudes and radial distances by use of static models of the magnetosphere. Static models (e.g., models which assume fixed magnetic and electric fields and then determine the drifts of the particles in equilibrium conditions) can be said to have originated with Alfven.[37] Current examples can be found in Refs. 37-45 for the magnetosphere and in Ref. 46 for the plasmasphere (note that these are time-independent models). Somewhat more recent examples can be found in Refs. 47-49. These models allow a direct comparison with observations because most were developed for the express purpose of understanding satellite data. As will also be discussed in this section, ionic composition models, which are based on assumed static or equilibrium conditions, can similarly be compared with observations.

Figure 18 illustrates typical trajectories for different energy particles under the combined influences of the Earth's magnetic and electric fields in the equatorial plane.[39] Similarly, McIlwain[41] has analyzed ATS-5 observations carefully and has generated a "best fit" to these particle observations by varying the electric field model. McIlwain has thereby succeeded in "dissecting" ATS-5 observations and tracing the particles back to their origins. However, he notes that his model, which assumes constant fields, cannot account for particle trapping since time-varying fields are necessary to trap fresh fluxes of particles into closed orbits.

Konradi et al.[43] have combined the Mauk and McIlwain[26] analytic equation [Eq. (9)] for the injection boundary with a static field model to generate quantitative models of the near-geosynchronous magnetosphere to account for the arrival of fresh plasma. Particles are either traced backward in time from the satellite orbits to determine their origin or assumed to originate on or anti-Earthward of the Mauk and McIlwain boundary and traced forward from that boundary to the desired satellite position. The computed particle distributions in the plasmasphere for various pitch angles are in good qualitative agreement with observations by the Explorer 45 satellite (apogee $5.19R_E$, perigee altitude 268 km). This implies that observations at or near geosynchronous orbit can indeed be used to predict observations elsewhere. Other model calculations of this type can be found in Refs. 45 and 47-50.

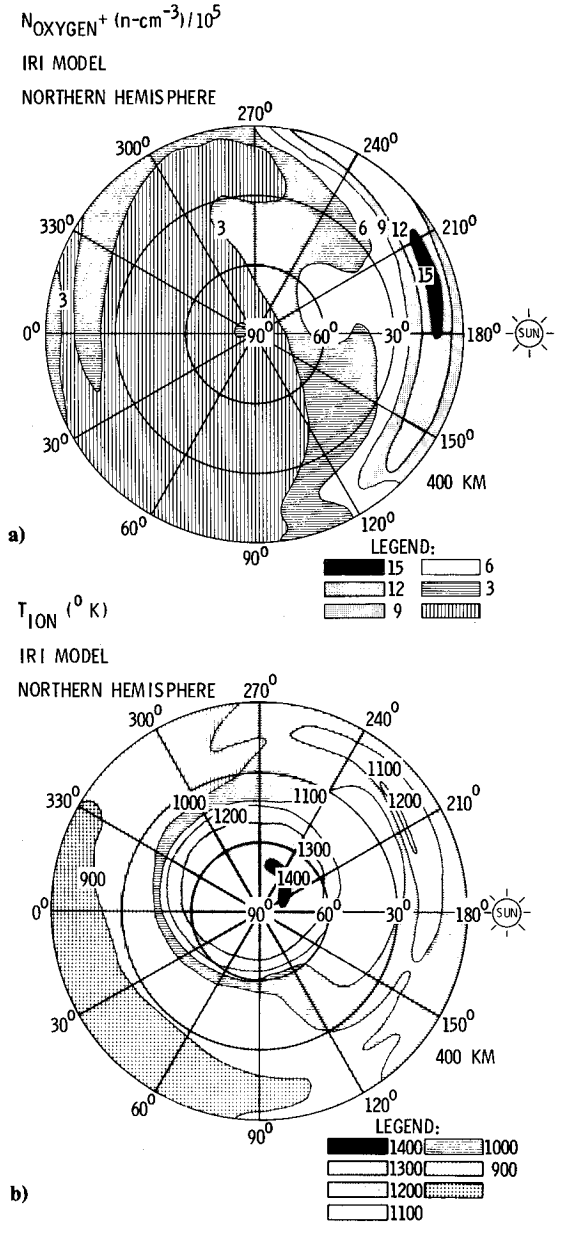

Fig. 16 Polar view of the oxygen ion environment at 400 km for December as predicted by the IRI model: a) oxygen ion density; b) oxygen ion temperature.

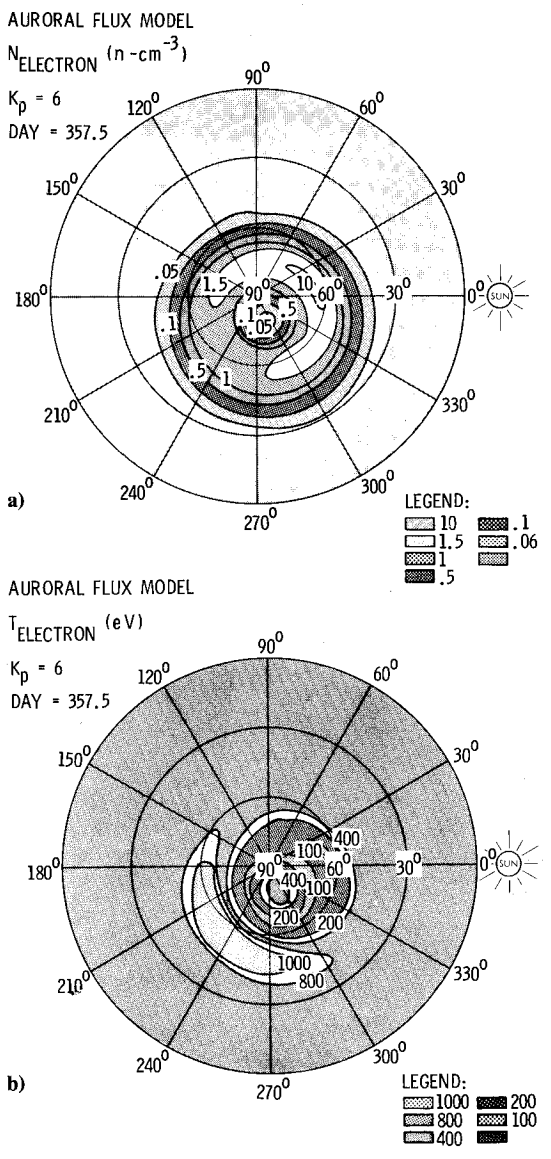

Fig. 17 Polar view of the auroral flux model adapted from AFGL and NOAA Auroral observations, altitude 800 km: a) oxygen ion density; b) oxygen ion temperature.

The major difference among these models is the source of the plasma injection particles; i.e., the plasma may be the result of inward convection from the Earth's magnetic tail, it may have been locally accelerated, or the source may have been the ionosphere. The actual answer is probably a combination of all of the above.

Numerous observations of the many different species of ions in the auroral and Van Allen domains are now available (see Table 1). Sharp et al.,[51] Fritz and Spjeldvik,[52] and Young et al.[53,54] report observations of kiloelectron and million electron-volt energy He^+, He^{++}, and O^+. In conjuction with these studies, Smith et al.,[55] and Spjeldvik and Fritz[56,57] (see also Refs. 58-60) have developed static models which consider the effects of diffusion, charge exchange, and various transport processes to account for the observations. For example, Smith et al.[55] compare their model decay times for a mixture of H^+, O^+ with observations from Explorer 45 for the energy range 6-25 keV. Other efforts[39,40,46] have resulted in models of the plasmasphere particle trajectories in the equatorial plane (Fig. 19).

The plasmasphere, as discussed previously, is part of the ionospheric domain. As such it is subject not only to particle drifts but to the diffusion of the ionospheric particles up along the magnetic field lines. Many models have been developed to account for this process in the exosphere and plasmasphere. Among these, a few of the better known are those of Refs. 61-63. Since these models do not account for the influences of electrostatic diffusion parallel to the magnetic field and the magnetic gradient force along the magnetic field line, they cannot be extended too far into the plasmasphere and essentially are limited to the topside ionosphere (or Shuttle region). More recent models have treated the problem of exospheric thermal plasma distributions along a magnetic field line in the plasmasphere[64,65] or over the polar caps[66,67] by explicitly including these effects. An example of these models is provided by Chiu et al.,[68] who have produced a comprehensive equilibrium model of plasmaspheric composition and density. Figure 20 is a comparison of their results for different boundary conditions for the topside ionosphere with observations. Since their model does not explicitly take into account local

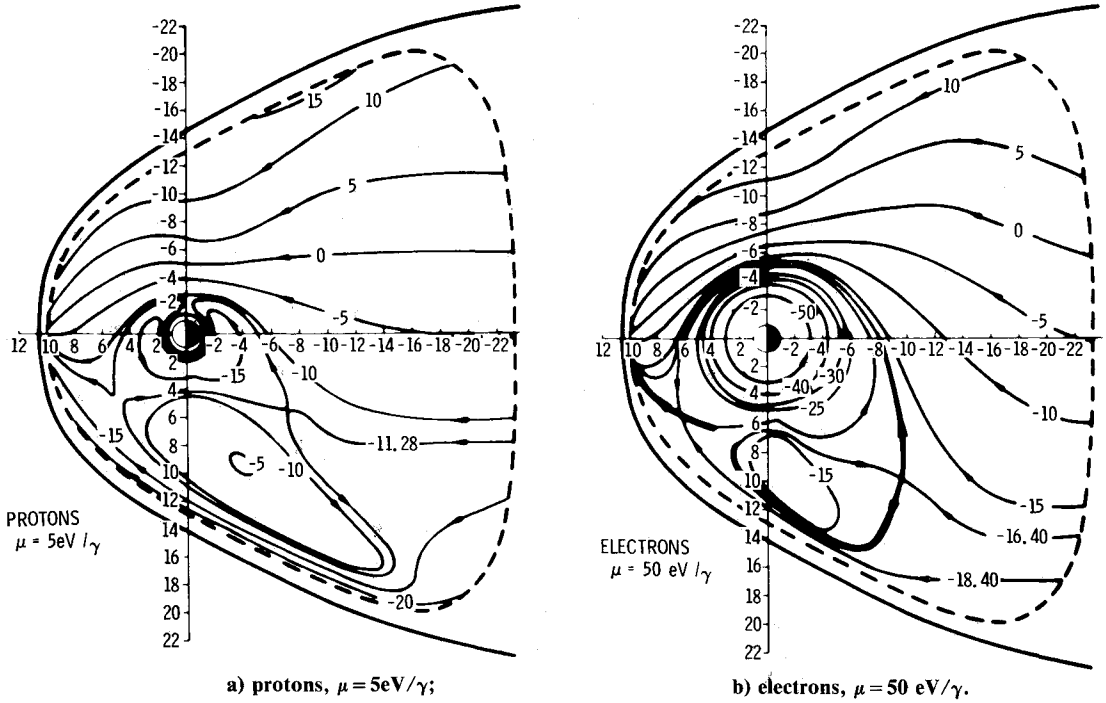

a) protons, $\mu = 5\text{eV}/\gamma$; b) electrons, $\mu = 50\ \text{eV}/\gamma$.

Fig. 18 Sample trajectories for protons and electrons; arrows indicate the particle flow directions (Ref. 39):

Table 2 Partial list of quantitative models users and the estimated applicability of the four model types to their needs[84]

		Model applicability			
User	Needs	Statistical	Analytic	Static	Time dependent
Department of Defense	Cumulative flux dosages	Satisfactory	Limited	Over defined	Over defined
NASA	Mission planning	Satisfactory	Moderate	Over defined	Over defined
Commercial	Satellite design and operation	Satisfactory	Satisfactory	Over defined	Over defined
	National Defense	Satisfactory	Satisfactory	Limited	Over defined
NOAA	Mission failure analysis	Satisfactory	Moderate	Over defined	Over defined
Air Force Air Weather Service	Forecasting	Satisfactory	Moderate	Moderate	Over defined
Department of Energy	Environment impact assessment	Limited	Limited	Satisfactory	Satisfactory
NASA	reference models	Satisfactory	Moderate	Satisfactory	Moderate
Scientific community	Ionospheric models	Limited	Limited	Satisfactory	Moderate
	Substorm modeling	Limited	Moderate	Moderate	Satisfactory
	Plasma dynamics	Limited	Limited	Moderate	Satisfactory
	Solar/terrestrial coupling	Limited	Limited	Moderate	Satisfactory

time, the bars on the observations represent the range in data due to this variable.

Time-Dependent Models

Time-dependent models, while ultimately the best way to study plasma variations along an arbitrary satellite orbit in the absence of actual data, are currently too cumbersome to be of use to the spacecraft charge modeler. Given the fact that most accurate spacecraft charging codes presently in use require large amounts of storage and run time, it is clear that the added burdens imposed by an accurate time-dependent plasma model would be prohibitive for most practical applications. Hence, only a few points relevant to quantitative modeling will be discussed here.

At present, time-dependent magnetospheric models can be loosely grouped into three categories: 1) static models to which a varying component such as the electric field is added in an ad hoc manner; 2) plasmadynamic models in which the interaction between the solar wind and the Earth's magnetic field are simulated using the magnetohydrodynamic models developed for plasma fusion studies[64] (because these models do not currently attempt to predict plasma variations in the near-Earth environment, they are not relevant to this study); and 3) self-consistent magnetospheric models which include coupling between the ionosphere and magnetosphere. Models of types 1 and 3 will be discussed below.

As indicated by McIlwain,[41] static models cannot account for the existence of injected plasma on closed drift paths because such particles are rapidly lost by various magnetospheric effects. Roederer and Hones[70] have developed an effective solution to this problem by adding a time-varying uniform dawn/dusk electric field and a localized azimuthal field to their static model.[38] The electric field is then adjusted to yield numerical results comparable with the ATS-5 data of DeForest and McIlwain.[6] A rise time of 10 min followed by a slow decay (2 h) was found to be necessary to account for the ATS-5 observations. Unfortunately, the model is limited to 90 deg pitch angles and energies above 1 keV. Smith et al.[71,72] have developed a similar model in which they assume a dipolar magnetic field and a time-varying convection electric field of the Volland-Stern type using the formalism of Ejiri et al.[73,74] In this model, the convection electric field is assumed to be described by a potential of the form:

$$\phi = A\,R^2 \sin\phi \tag{12}$$

where ϕ is the local time dependence (0 at midnight) and R the radial distance from Earth. A is taken to be of the form[75]:

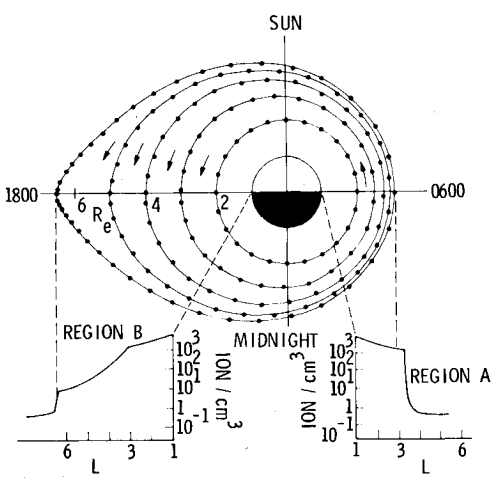

Fig. 19 Motion of flux tubes in the plasmasphere.[46] The distance between dots gives the approximate drift distance of the flux tubes in 1 h.

$$A = \frac{0.045}{(1 - 0.159\,K_p + 0.009\,K_p^2)^3} \tag{13}$$

Although the Roederer-Hones model is successful in fitting the ATS-5 data and the Smith et al. model in demonstrating time variations in the particle fluxes, they are not intended to be self-consistent; i.e., the fields that the particles themselves generate and the background fields are not constrained to agree. The Rice University group, under R.A. Wolf, has carried out a systematic development program aimed at ultimately developing a self-consistent three-dimensional model of the magnetospheric storm processes. Only a very sketchy description will be given here, and the reader is referred to the most recent papers published by the Rice University group.[76-78]

As originally outlined by Vasyliunas[2] the method starts with a model of the Earth's electric and magnetic fields and calculates the plasma distribution and pressure. The currents perpendicular to the magnetic field are calculated from the pressure gradients. The divergence of these currents determines the field-aligned currents flowing between the magnetosphere and ionosphere. The assumption of closed loops permits calculation of the electric fields in the ionosphere. The ionospheric electric fields are mapped back into the magnetosphere, and the magnetospheric plasma is then allowed to drift in response to this electric field and redistribute itself. By repeating the process the program steps forward in time. The model[76] has been used to simulate the plasma flows and field variations seen in space and at the Earth's surface during actual substorms.

Versions of the Rice University model also have been applied to calculate the drifts in the plasmasphere. Early results of this modeling[79] predicted that the plasmasphere. boundary would become severely distorted during geomagnetic storms so that plasma tails, as illustrated in Fig. 21, would be generated. Such regions have been observed[80] subsequently and illustrate the complex structure of time-dependent magnetosphere as compared with static or "mean" models.[81,82] A primary feature of the plasmasphere models developed in these latter papers is a simple analytic expression for the equatorial convection E field as a function of K_p. A typical formula for the dawn-dusk amplitude[83] is

$$E = 0.13/(1 - 0.1\,K_p)^2 \text{ mV/m} \tag{14}$$

Varying K_p causes the electric field and particle drifts to vary, generating the plasma tails observed in the data.

Engineering Models

Introduction

It is clear that there is no straightforward answer to the practical question: "What type of environmental model should I use to calculate spacecraft charging?" As should be obvious, each such calculation must involve a complex tradeoff between accuracy of representation and simplicity (or, in many cases, low cost). The purpose of the preceding discussion has been to illustrate the spectrum of choices available to the spacecraft charging modeler. In this concluding subsection, practical guidelines on how to choose the proper type of model will be suggested.

As a first step in helping to determine the proper match between user and model, Table 2 assesses potential users, their needs, and the applicability of the particular model type to those needs. The list of users is far from complete, but, even so, a variety of possible applications were considered in its construction. For example, statistical models are particularly useful in any problem requiring long-term integration of plasma fluxes such as for dosage calculations. Since, at present, geomagnetic activity cannot be forecast accurately, the best that can be done is to predict the probability of particular fluxes being observed; hence, statistical models are useful in

this application as well. On the other hand, analytic models can be used to simulate the magnetospheric variations during substorms or the conditions at the beginning of a storm for input into more sophisticated models. They can be used to generate estimates of plasma variations efficiently under a variety of conditions. Specific "baseline" examples of these two model types will be suggested subsequently.

Static models are useful in applications where a limited number of observations are available. As a possible application, measurements from three evenly spaced geosynchronous satellites could be extrapolated to other spatial positions to give a three-dimensional, real-time picture of the state of the magnetosphere. Ultimately, however, a time-dependent model in which the pertinent physical variables are properly included would allow detailed predictions and extrapolations to all orbital regimes and conditions. Such a model, particularly an efficient and accurate model, is still far in the future and, for many of the users listed in Table 2, would give more information than is required and would certainly cost more than the increased accuracy of representation would merit. Hence, no

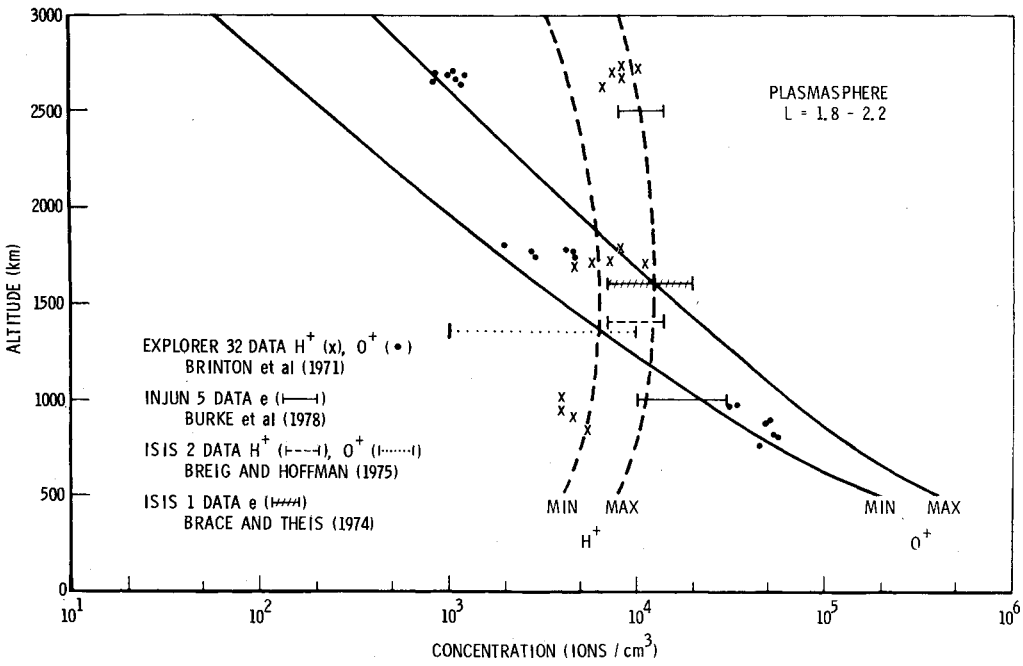

Fig. 20 Comparison between in situ observations of the topside ionosphere and plasmasphere model of Chiu et al.[68] for two different boundary conditions at 500 km (particle densities at boundaries have been doubled between MIN and MAX).

Table 3 Worst-case geosynchronous environments[a]

	Source					
	Deutsch (1981)		Mullen et al. (1981)		Mullen and Gussenhoven (1982)	
	Date					
	Day 178, 1974		Day 114, 1979		—	
	Spacecraft					
	ATS-6		SCATHA		SCATHA	
Parameter	Electrons	Ions	Electrons	Ions	Electrons	Ions
Number density, ⟨ND⟩, cm^{-3}	1.12	0.245	0.900	2.30	3.00	3.00
Current density, ⟨J⟩, nA cm^{-2}	0.410	0.025	0.187	0.795×10^{-2}	0.501	0.0159
Energy density, ⟨ED⟩, eV cm^{-3}	0.293×10^{5}	0.104×10^{5}	0.960×10^{4}	0.190×10^{5}	0.240×10^{5}	0.370×10^{5}
Energy flux, ⟨EF⟩, eV cm^{-2} s^{-1} sr^{-1}	0.264×10^{14}	0.298×10^{12}	0.668×10^{13}	0.430×10^{13}	0.151×10^{14}	0.748×10^{12}
Number density for population 1, N_1, cm^{-3}						
Parallel	—	0.882×10^{-2}	0.200	1.60	1.00	1.10
Perpendicular	—	—	0.200	1.10	0.800	0.900
Temperature for population 1, T_1, eV						
Parallel	—	0.111×10^{3}	0.400×10^{3}	0.300×10^{3}	0.600×10^{3}	0.400×10^{3}
Perpendicular	—	—	0.400×10^{3}	0.300×10^{3}	0.600×10^{3}	0.300×10^{3}
Number density for population 2, N_2, cm^{-3}						
Parallel	1.22	0.236	0.600	0.600	1.40	1.70
Perpendicular	—	—	2.30	1.30	1.90	1.60
Temperature for population 2, T_2, eV						
Parallel	0.160×10^{5}	0.295×10^{5}	0.240×10^{5}	0.260×10^{5}	0.251×10^{5}	0.247×10^{5}
Perpendicular	—	—	0.248×10^{5}	0.282×10^{5}	0.261×10^{5}	0.256×10^{5}
Average temperature, T_{av}, eV	0.160×10^{5}	0.284×10^{5}	0.770×10^{4}	0.550×10^{4}	0.533×10^{4}	0.822×10^{4}
Root-mean-square temperature, T_{rms}, eV	0.161×10^{5}	0.295×10^{5}	0.900×10^{4}	0.140×10^{5}	0.733×10^{4}	0.118×10^{5}

[a]The moments, T_{av}, and T_{rms} are averaged over all angles. The SCATHA two-Maxwellian parameters are for fluxes parallel and perpendicular to the magnetic field. ATS-6 two-Maxwellian parameters are averaged over all directions.

discussion of these models will be included in this sub-section.

Baseline Models

As demonstrated by Table 2, there is a real need for a "baseline" statistical or analytic model of the space environment for studying spacecraft charging effects on space systems. Careful consideration of user needs indicates that, as a minimum, the model must give representative values for the plasma density and temperature as a function of position, local time, and geomagnetic activity. For most statistical purposes, the frequency-of-occurrence plots of geosynchronous parameters in Fig. 4 are sufficient for spacecraft charging studies where rapid time variations are not important. These frequency-of-occurrence plots yield information on the median values of the number density and temperature and an estimate of the ranges to be expected. The ionic composition estimates given in Table 1, while only intended to indicate ranges, should also be adequate for such applications.

Within the ionospheric domain, the suggested baseline composition/temperature profiles for day, night and the solar cycle are presented in Figs. 9-11 for 60-1000 km.[24] For applications requiring more detail (such as the Shuttle or space station), the IRI model is recommended. As discussed, details of the ionic composition between 1000 km and geosynchronous orbit (GEOS-1 observations should be used to estimate the low-latitude ion variations in this region) and in the polar cap domain became available only recently. In the interim, predictions of the Ching and Chiu models for total charge content or the theoretical models of ion content discussed earlier, particularly over the polar caps, can be employed. The models of Young et al.[65] at low latitudes and Sojka et al.[66] over the polar caps are examples.

"Baseline" time variations are difficult to model due to the many nonadiabatic processes taking place in the magnetosphere on time scales of minutes or less. Even so, for spacecraft charge modeling it is recommended that the models of Su and Konradi[5] or Garrett and DeForest[8] and subsequent versions which define plasma observations in terms of geomagnetic and local time variations be used to simulate typical variations. The recent SCATHA P78-2 data atlas[14] also provides insights in this area. Substorm-specific variations for the electrons in the midnight local time quadrant can be estimated using Fig. 13 and similar figures although it should be remembered that this represents an "average" substorm rather than a worst case. Young et al.[54] have presented extensive plots of average variations of ions with geomagnetic activity, solar ultraviolet, and local time that can be used to supplement these models. As yet no analytic models of the polar cap regime exist which explicitly include rapid time variations due to geomagnetic activity and could be used for "baseline." The IRI model, to the extent that it includes sunspot number, can be used to simulate mean variations, however, in local time and longitude of the ionosphere for low to moderate levels of activity.

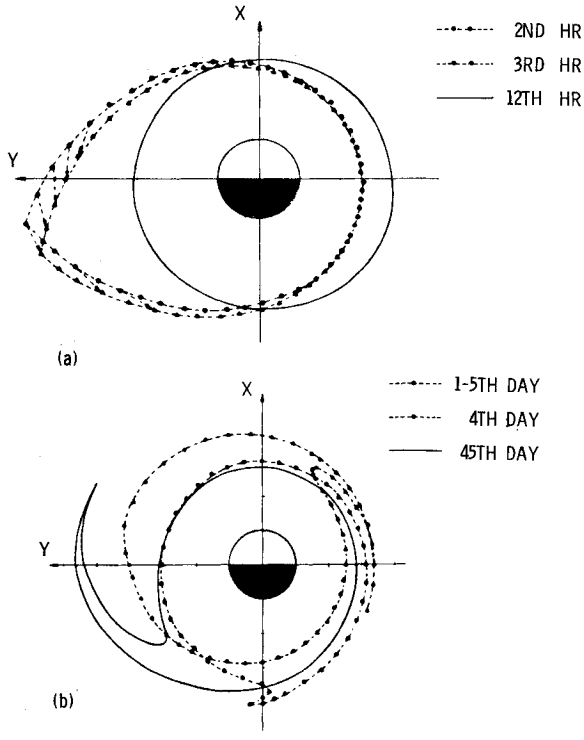

Fig. 21 Distortion of plasmapause following factor of 2 decrease in the convection electric field at time $t=0$.[79]

"Worst-Case" Models

In many spacecraft charging calculations it is desired to have a "worst-case" scenario for design studies. At this writing, several such models have been developed for geosychronous orbit, which represents, for spacecraft charging, the most severe environment. Table 3 lists several of these "worst-case" environments in terms of the plasma moments and Maxwell-Boltzmann components.[85,86,14] It is suggested that each of these be tried for a given design, since different vehicles may respond differently to each of the environments. Further, the reader is cautioned that particle flux anisotropies will affect the results for different orientations of the vehicle. Similarly, ionic composition is believed to influence the details of the spacecraft charging process. However, the examples in Table 3 should be adequate for most practical cases.

Missing from Table 3 is an estimate of the percentage of time that a satellite might expect to spend in such an environment. Examples of such estimates are those for the current and temperature.[87-89] Here it is noted that, given the durations of the ATS-5, ATS-6, and SCATHA missions, a satellite would spend only about one to two days total in 11 yr (one solar cycle) in an environment as severe as those of Table 3.

Conclusions

In this paper, the authors have attempted to summarize the basic features of the near-Earth, 0-100-keV plasma environment. A number of different types of models of that environment have been described with emphasis on those models of potential value to the spacecraft designer. Although it is clear that a detailed knowledge of the plasma environment and, in particular, of the plasma distribution function is required for accurate modeling of actual spacecraft charging effects,[90] simple representations in terms of the Maxwell-Boltzmann distribution function were found, when compared with user needs, to be useful for most design purposes. Therefore, as a supplement to the detailed models presented in the first part of the paper, specific recommendations of baseline and "worst case" models for use in calculating spacecraft charging were presented. In closing, it is hoped that this information will prove useful both to those desiring a general overview of the near-Earth plasma environment and to those requiring only that information necessary to determine the effects of spacecraft charging on their mission—the end to which this paper was written.

Acknowledgments

The research described in this paper was carried out by the Jet Propulsion Laboratory, California Institute of Technology, under Contract NAS 7-918 and sponsored jointly by the Air Force Geophysics Laboratory and the National Aeronautics and Space Administration.

References

[1]Frank, L. A., "Magnetospheric and Auroral Plasmas: A Short Survey of Progress," *Reviews of Geophysics and Space Physics*, Vol. 12, 1975, p. 974.

[2]Vasyliunas, V. M., "Mathematical Models of Magnetospheric Convection and Its Coupling to the Ionosphere," *Particles and Fields in the Magnetosphere,* edited by B. M. McCormac, D. Reidel, Hingham, Mass., 1970.

[3]Vasyliunas, V. M, "Magnetospheric Plasma," *Solar Terrestrial Physics 1970, Proceedings of the International Symposium,* USSR, May 1970, Pt. III, edited by E. R. Dyer, D. Reidel, Hingham, Mass., 1972.

[4]Chan, K. W., Sawyer, D. M., and Vette, J. I., "Model of the Near-Earth Plasma Environment and Application to the ISEE-A and −B Orbit," Goddard Space Flight Center, Greenbelt, Md., NSSDC/WDC-A-RS 7701, July 1977.

[5]Su, S-Y. and Konradi, A., "Description of the Plasma Environment at Geosynchronous Altitude," NASA Johnson Tech. Note P-10, 1977.

[6]DeForest, S. E. and McIlwain, C. E., "Plasma Clouds in the Magnetosphere," *Journal of Geogphysical Research,* Vol. 76, 1971, p. 3587.

[7]Garrett, H. B., "Modeling of the Geosynchronous Orbit Plasma Environment, 1," Air Force Geophysics Lab., Bedford, Mass., AFGL-TR-0288, 1977.

[8]Garrett, H. B. and DeForest S. E., "An Analytical Simulation of the Geosynchronous Plasma Environment," *Planetary and Space Science,* Vol. 27, 1979, pp. 1101-1109.

[9]Mullen, E. G., Hardy, D. A., Garrett, H. B., and Whipple, E. C., "P78-2 SCATHA Environmental Data Atlas," *Spacecraft Charging Technology,* 1980, NASA CP 2182/AFGL-TR-81-0270, 198lb, pp. 802-813.

[10]Garrett, H. B., Schwank, D. C., and DeForest, S. E., "A Statistical Analysis of the Low-Energy Geosynchronous Plasma Environment—I. Electrons," *Planetary and Space Science,* Vol. 29, 1981a, pp. 1021-1044.

[11]Garrett, H. B., Schwank, D. C., and DeForest, S. E., "A Statistical Analysis of the Low-Energy Geosynchronous Plasma Environment—II. Protons," *Planetary and Space Science,* Vol. 29, 198lb, pp. 1045-1060.

[12]Geiss, J. et. al., "Dynamics of Magnetospheric Ion Composition as Observed by the GEOS Mass Spectrometer," paper presented at 13th ESLAB Symposium, European Space Agency, Innsbruck, Austria, June 1978.

[13]Young, D. T., "Ion Composition Measurements in Magnetospheric Modeling," *Quantitative Modeling of the Magnetospheric Processes, Geogphysics Monograph Series,* Vol. 21, edited by W. P. Olson, AGU, Washington, D. C., 1979, pp. 340-363.

[14]Mullen, E.G. and Gussenhoven, M.S., "SCATHA Environmental Atlas," AFGL-TR-0002, 1983.

[15]Frank, L. A., "On the Extraterrestrial Ring Current During Geomagnetic Storms," *Journal of Geophysical Research,* Vol. 72, 1967, p. 3753.

[16]Roederer, J. G., "Dynamics of Geomagnetically Trapped Radiation," *Physics and Chemistry in Space,* Vol. 2, edited by J. G. Roederer and J. Zahringer, Springer-Verlag, New York, 1970.

[17]Carpenter, D. L., "Whistler Studies of the Plasmapause in the Magnetosphere: 1,—Temporal Variations in the Position of the Knee and Some Evidence on Plasma Motions Near the Knee," *Journal of Geophysical Research,* Vol. 71, 1966, p. 693.

[18]Chappell, C. R., "Recent Satellite Measurements of the Morphology and Dynamics of the Plasmasphere," *Reviews of Geophysics and Space Physics,* Vol. 10, 1972, p. 951.

[19]Carpenter, D. L. and Park, C. G., "On What Ionospheric Workers Should Know About the Plasmapause-Plasmasphere," *Reviews of Geophysics and Space Physics,* Vol. 11, 1973, p. 133.

[20]Gringauz, K. I. and Bezrukikh, V. V., "Plasmasphere of the Earth (Review)," *Geomagnetics and Aeronautics,* Vol. 17, 1977, p. 523.

[21]Park, C. G., Carpenter, D. L., and Wiggin, D. B., "Electron Density in the Plasmasphere: Whistler Data on Solar Cycle, Annual, and Diurnal Variations," *Journal of Geophysical Research,* Vol. 83, 1978, p. 3137.

[22]Gringauz, K. I. and Bezrukikh, V. V., "Asymmetry of the Earth's Plasmasphere in the Direction Noon-Midnight from Prognoz and Prognoz-2 Data," *Journal of Atmospheric and Terrestrial Physics,* Vol. 38, 1976, p. 1071.

[23]Ahmed, M., Sagalyn, R. C., Wildman, P. J. L., and Burke, W. J., "Topside Ionospheric Trough Morphology: Occurrence Frequency and Diurnal, Seasonal, and Altitude Variation," *Journal of Geophysical Research,* Vol. 84, 1970, p. 489.

[24]Carrigan, A. L. and Skrivaneck, R. A., "The Aerospace Environment," AFCRL Chart, 1974.

[25]DeForest, S. E., and Wilson, A. R., "A Preliminary Specification of the Geosynchronous Plasma Environment," Defense Nuclear Agency, Washington, D. C., Rept. DNA 39515, 1976.

[26]Mauk, B. H. and McIlwain, C. E., "Correlation of K_p with the Substorm Plasma Sheet Boundary," *Journal of Geophysical Research* Vol. 79, 1974, p. 3193.

[27]Freeman, J. W., "K_p Dependence of the Plasma Sheet Boundary," *Journal of Geophysical Research,* Vol. 79, 1974, p. 4315.

[28]Kivelson, M. G. and Southwood, D.J., "Approximations for the Study of Drift Boundaries in the Magnetosphere," *Journal of Geophysical Research,* Vol. 80, 1975, p. 3528.

[29]Kivelson, M. G., "Magnetospheric Electric Fields and Their Variations with Geomagnetic Activity," *Reviews of Geophysics and Space Physics,* Vol. 14, 1976, p. 189.

[30]Lemaire, J., "Steady State Plasmapause Positions Deduced from McIlwain's Electric Field Models," *Journal of Atmospheric and Terrestrial Physics,* Vol. 38, 1976, p. 1041.

[31]Ching, B. K. and Chiu, Y. T., "A Phenomenological Model of Global Ionospheric Electron Density in the E-, Fl- and F2-Regions," *Journal of Atmospheric and Terrestrial Physics,* Vol. 35, 1973, pp. 1615-1630.

[32]Chiu, Y. T., "An Improved Phenomenological Model of Ionospheric Density," *Journal of Atmospheric and Terrestrial Physics,* Vol. 37, 1975, pp. 1563-1570.

[33]"International Reference Ionosphere—IRI 79," edited by J. V. Lincoln and R. O. Conkright, World Data Center A, Boulder, Colo., Rept. UAG-82, Nov. 1981.

[34]Rawer, K., Minnis, C. M., Serafimov, K. B., "Towards an Improved International Reference Ionosphere," *Advances in Space Research,* Vol. 4, No. 1, 1984.

[35]Hardy, D. A., "The Worst Case Charging Environment," *Proceedings of the Air Force Geophysics Laboratory Workshop on Natural Charging of Large Space Structures in Near Earth Polar Orbit: 14-15 September 1982,* edited by R. C. Sagalyn, D. E. Donatelli, and I. Michael, AFGL-TR-83-0046, 1983, pp. 141-155.

[36]Evans, D., private communications. NOAA, Boulder, Colo., 1985.

[37]Alfven, H., "A Theory of Magnetic Storms and of the Aurorae," *Proceedings of the Royal Swedish Academy of Sciences,* Stockholm, 1939; (reprinted in *EOS Transactions of AGU,* Vol. 51, 1970, p. 180).

[38]Roederer, J.G., and Hones, E.W. Jr., "Electric Field in the Magnetosphere as Deduced from Asymmetries in the Trapped Particle Flux," *Journal of Geophysical Research,* Vol. 75, 1970, p. 3923.

[39]Wolf, R. A., "Effects of Ionospheric Conductivity on Convective Flow of Plasma in the Magnetosphere," *Journal of Geophysical Research,* Vol. 75, 1970, p. 4677.

[40]Chen, A. J., "Penetration of Low-Energy Protons Deep into the Magnetosphere," *Journal of Geophysical Research,* Vol. 75, 1970, p. 3848.

[41]McIlwain, C. E., "Plasma Convection in the Vicinity of the Geosynchronous Orbit," *Earth's Magnetospheric Processes,* edited by B. M. McCormac, D. Reidel, Hingham, Mass., 1972, pp. 268-279.

[42]Williams, D. J., Barfield, J. N., and Fritz, T. A., "Initial Explorer 45 Substorm Observations and Electric Field Considerations," *Journal of Geophysical Research,* Vol. 79, 1974, p. 554.

[43]Konradi, A., Semar, C. L., and Fritz, T. A., "Substorm-Injected Protons and Electrons and the Injection Boundary Model," *Journal of Geophysical Research,* Vol. 80, 1975, p. 543.

[44]Kavanagh Jr., L. D., Freeman Jr., J. W., and Chen A. J., "Plasma Flow in the Magnetosphere," *Journal of Geophysical Research,* Vol. 73, 1968, p. 5511.

[45]Walker, R. J. and Kivelson, M. G., "Energization of Electrons at Synchronous Orbit by Substorm-Associated Cross-Magnetospheric Electric Fields," *Journal of Geophysical Research,* Vol. 80, 1975, p. 2074.

[46]Chappell, C. R., Harris, K.K., and Sharp, C. W., "The Morphology of the Bulge of the Plasmasphere," *Journal of Geophysical Research,* Vol. 75, 1970, p. 3848.

[47]Cowley, S. W. H., "Energy Transport and Diffusion," *Physics of Solar Planetary Environments,* Vol. 2, edited by D. J. Williams, AGU, Washington, D. C., 1976.

[48]Cowley, S. W. H. and Ashour-Abdalla, M., "Adiabatic Plasma Convection in a Dipole Field: Electron Forbidden-Zone Effects for a Single Electric Field Model," *Planetary and Space Science,* Vol. 24, 1976a, p. 805.

[49]Cowley, S. W. H. and Ashour-Abdalla, M., "Adiabatic Plasma Convection in a Dipole Field: Proton Forbidden-Zone Effects for a Single Electric Field Model," *Planetary and Space Science,* Vol. 24, 1976b, p. 821.

[50]Southwood, D. J. and Kivelson, M. G., "An Approximate Analytic Description of Plasma Bulk Parameters and Pitch Angle Anisotrophy Under Adiabatic Flow in a Dipolar Magnetospheric Field," *Journal of Geophysical Research,* Vol. 80, 1975, p. 2069.

[51]Sharp, R. D., Shelley, E. G., and Johnson R. G., "A Search for Helium Ions in the Recovery Phase of a Magnetic Storm," *Journal of Geophysical Research,* Vol. 82, 1977, p. 2361.

[52]Fritz, T. A., and Spjeldvik, W. N., "Observations of Energetic Radiation Belt Helium Ions at the Geomagnetic Equator During Quiet Conditions," *Journal of Geophysical Research,* Vol. 83, 1978, p. 2579.

[53]Young, D. T., Geiss, J., Balsiger, H., Eberhardt, P., Ghielmetto, A., and Rosenbauer, H., "Discovery of He^{2+} and O^{2+} Ions of Terrestrial Origin in the Outer Magnetosphere," *Geophysical Research Letters,* Vol. 4, 1977, p. 561.

[54]Young, D. T., Balsiger, H., and Geiss, J., "Correlations of Magnetospheric Ion Composition with Geomagnetic and Solar Activity," *Journal of Geophysical Research,* Vol. 87, 1982, pp. 9077-9096.

[55]Smith, R. H., Bewtra, N. K., and Hoffman, R. A., "Interference of the Ring Current Ion Composition by Means of Charge Exchange Decay," NASA TM-79611, 1978a.

[56]Spjeldvik, W. N. and Fritz, T. A., "Energetic Ionized Helium in the Quiet Time Radiation Belts: Theory and Comparison with Observation," *Journal of Geophysical Research,* Vol. 83, 1978a, p. 1654.

[57]Spjeldvik, W. N. and Fritz, T. A. "Theory for Charge States of Energetic Oxygen Ions in the Earth's Radiation Belts," *Journal of Geophysical Research,* Vol. 83, 1978b, p. 1583.

[58]Tinsley, B. A., "Evidence That the Recovery Phase Ring Current Consists of Helium Ions," *Journal of Geophysical Research,* Vol. 81, 1976, p. 6195.

[59]Lyons, L. R. and Evans, D. S., "The Inconsistency Between Proton Charge Exchange and the Observed Ring Current Decay," *Journal of Geophysical Research,* Vol. 81, 1976, p. 6297.

[60]Freeman, J. W., Hills, H. K., and Reiff, H., "Heavy Ion Circulation in the Earth's Magnetosphere," *Geophysical Research Letters,* Vol. 4, 1977, p. 195.

[61]Angerami, J. J. and Thomas, J. O., "Studies of Planetary Atmosphere: 1. The Distribution of Electrons and Ions in the Earth's Exosphere," *Journal of Geophysical Research,* Vol. 69, 1964, p. 4537.

[62]Schunk, R. and Walker, J. C. G., "Thermal Diffusion in the Topside Ionosphere for Mixtures Which Include Multiply Charged Ions," *Planetary and Space Science,* Vol. 17, 1969, p. 853.

[63]Mayr, H. G., Fontheim, E. G., Brace, L. H., Brinton, H. C., and Taylor Jr., H. A., "A Theoretical Model of the Ionosphere Dynamics with Interhemispheric Coupling," *Journal of Atmospheric and Terrestrial Physics,* Vol. 34, 1972, p. 1659.

[64]Lemaire,J. and Scherer, M., "Exospheric Models of the Topside Ionosphere," *Space Science Reviews,* Vol.15, 1974, p. 591.

[65]Young, E. R., Torr, D. G., Richards, P., and Nagy, A. F., "A Computer Simulation of the Midlatitude Plasmasphere and Ionosphere," *Planetary and Space Science,* Vol. 28, 1980, pp. 881-893.

[66]Sojka, J. J., Raitt, W. J., and Schunk, R. W., "Theoretical Predictions for Ion Composition in the High-Latitude Winter F-Region for Solar Minimum and Low Magnetic Activity," *Journal of Geophysical Research,* Vol. 86, 1981, pp. 2206-2216.

[67]Singh, N. and Schunk, R. W., "Numerical Calculations Relevant to the Initial Expansion of the Polar Wind," *Journal of Geophysical Research,* Vol. 87, 1982, pp. 9154-9170.

[68]Chiu, Y. J., Luhmann, J. G., Ching, B. K., and Boucher Jr., D. J., "An Equilibrium Model of Plasmaspheric Composition and Density," *Journal of Geophysical Research,* Vol. 84, 1979, pp. 909-916.

[69]Leboeuf, J. N., Tajima, T., Kennel, C. F., and Dawson, J. M., "Global Magnetohydrodynamic Simulation of the Two-Dimensional Magnetosphere," *Quantitative Modeling of Magnetospheric Processes,* edited by W. P., Olson, AGU, Washington, D. C., 1979, pp. 536-556.

[70]Roederer, J. G. and Hones Jr., E. W., "Motion of Magnetospheric Particle Clouds in a Time-Dependent Electric Field Model," *Journal of Geophysical Research,* Vol. 79, 1974, p. 1432.

[71]Smith, R. H., Hoffman, R. A., and Bewtra, N. K., "A Visual Description of the Dynamical Nature of Magnetospheric Particle Convection in a Time-Varying Electric Field (Abstract)," *EOS Transactions of AGU,* Vol. 59, 1978b, p. 361.

[72]Smith, R. H., Bewtra, N. K., and Hoffman, R. A., "Motions of Charged Particles in the Magnetosphere Under the Influence of Time-Varying Large Scale Convection Electric Field," *Quantitative Modeling of the Magnetospheric Processes, Geophysics Monograph Series,* Vol. 21, edited by W. P. Olson, AGU, Washington, D. C., 1979, pp. 513-535.

[73]Ejiri, M., "Trajectory Traces of Charge Particles in the Magnetosphere," *Journal of Geophysical Research,* Vol. 83, 1978, p. 4798.

[74]Ejiri, M., Hoffman, R. A., and Smith, P. H., "The Convection Electric Field Model for the Magnetosphere Based on Explorer 45 Observations," *Journal of Geophysical Research,* Vol. 83, 1978, p. 4811.

[75]Grebowsky, J. M. and Chen, A. J., "Effects of Convection Electric Field on the Distribution of Ring Current Type Protons," *Planetary and Space Science,* Vol. 23, 1975, p. 1045.

[76]Harel, M. et al., "Quantitative Simulation of a Magnetospheric Substorm: 1. Model Logic and Overview," *Journal of Geophysical Research,* Vol. 86, 1981a, pp. 2217-2241.

[77]Harel, M. et al., "Quantitative Simulation of a Magnetospheric Substorm: 2. Comparison with Observations," *Journal of Geophysical Research,* Vol. 86, 1981b, pp. 2242-2260.

[78]Spiro, R. W., Harel, M., Wolf, R. A. and Reiff, P. H., "Quantitative Simulation of a Magnetospheric Substorm: 3. Plasmaspheric Electric Fields and Evolution of the Plasmapause," *Journal of Geophysical Research,* Vol. 86, 1981, pp. 2261-2272.

[79]Chen, A. J., and Wolf, R. A., "Effects on the Plasmasphere of a Time-Varying Convection Electric Field," *Planetary and Space Science,* Vol. 20, 1972, p. 483.

[80]Chappell, C. R., "Detached Plasma Regions in the Magnetosphere," *Journal of Geophysical Research,* Vol. 79, 1974, p. 1861.

[81]Chen, A. J. and Grebowsky, J. M., "Plasma Tail Interpretations of Pronounced Detached Plasma Regions Measured by OGO 5," *Journal of Geophysical Research,* Vol. 79, 1974, p. 3851.

[82]Chen, A. J., Grebowsky, J. M., and Taylor Jr., H. A., "Dynamics of Mid-Latitude Light Ion Trough and Plasma Tails," *Journal of Geophysical Research,* Vol. 80, 1975, p. 968.

[83]Grebowsky, J. M., Tulunay, Y., and Chen, A. J., "Temporal Variations in the Dawn and Dusk Midlatitude Trough and Plasmapause Position," *Planetary and Space Science,* Vol. 22, 1974, p.1089.

[84]Garrett, H. B., "Review of Quantitative Models of the 0- to 100-keV Near-Earth Plasma," *Reviews of Geophysical and Space Science,* Vol. 17, 1979, pp. 397-416.

[85]Deutsch, M.-J., "A 'Worst Case' Charging Environment: Day 178, 1974," *Journal of Spacecraft and Rockets,* Vol. 19, 1982, pp. 473-477.

[86]Mullen, E. G., Gussenhoven, M. S., and Garrett, H. B., "A 'Worst Case' Spacecraft Environment as Observed by SCATHA on 24 April 1979," AFGL-TR-0231, 1981a.

[87]Stevens, N. J., Lovell, R. R., and Purvis, C. K., "Provisional Specification for Satellite Time in a Geomagnetic Substorm Environment," *Proceedings of the Spacecraft Charging Conference,* Air Force Geophysics Lab., Bedford, Mass., AFGL-TR-77-0051/NASA-TMX-73537, 1977, pp. 735-744.

[88]DeForest, S. E., "Specification of the Geosynchronous Plasma Environment," Air Force Geophysics Lab., Bedford, Mass., AFGL-TR-77-0031, 1977.

[89]Purvis, C.K., Garrett, H. B., Whittlesey, A. C., and Stevens, N. J., "Design Guidelines for Assessing and Controlling Spacecraft Charging Effects," NASA TP-2361, Sept. 1984.

[90]Garrett, H. B., "The Charging of Spacecraft Surfaces," *Reviews of Geophysics and Space Physics,* Vol. 19, 1981c, pp. 577-616.